Available online at www.sciencedirect.com

ScienceDirect

Current Opinion in Electrochemistry

Review Article

Correlative co-located electrochemical multi-microscopy

Daniel Martín-Yerga, Patrick R. Unwin, Dimitrios Valavanis and Xiangdong Xu

Abstract

Correlative co-located electrochemical multi-microscopy is transforming our understanding of property–function relationships in electrode materials. By coupling scanning electrochemical cell microscopy (SECCM) with complementary characterization techniques applied to identical locations of a surface, we can now unravel the intricate interplay between various physicochemical properties of electrode materials and interfaces and their impact on electrochemical phenomena, with high spatial resolution. This review explores recent advances in this correlative approach to showcase how it can reveal major new insights into the activity of materials and interfaces. Applications span diverse electrochemical fields, including energy conversion and storage, sensing, and corrosion science. We also envision future developments that will open up new possibilities for rational materials design, accelerated mechanistic understanding, and automated materials discovery.

Addresses

Department of Chemistry, University of Warwick, CV4 7AL Coventry, UK

Corresponding author: Martín- Yerga, Daniel (daniel.martin-yerga@warwick.ac.uk)

Current Opinion in Electrochemistry xxxx, **xxx**:xxx

This review comes from a themed issue on **Surface Electrochemistry (2024)**

Edited by **Dongping Zhan** and **Yanxia Chen**

For a complete overview see the Issue and the Editorial

Available online xxx

https://doi.org/10.1016/j.coelec.2023.101405

Keywords

Correlative electrochemical multi-microscopy, Scanning electrochemical cell microscopy, Property–function relationships, Single-entity electrochemistry.

Introduction

Unraveling the intricate interplay between the physicochemical properties of materials and their impact on electrochemical behavior is critical to advance our fundamental knowledge of interfacial electrochemical phenomena. A clear understanding of property–function (e.g., structure-activity, which is the main focus herein) relationships in electrode components enables a bottom-up approach for their rational design and integration, optimized for applications in energy conversion and storage, electrocatalysis, sensing, electrosynthesis, and corrosion resistance. Traditional approaches to explore property–function relationships in electrode materials have relied heavily on macroscopic electrochemical characterization, which provides only an average representation of the material, overlooking inherent heterogeneity. In contrast, *correlative co-located electrochemical multi-microscopy* offers a more complete description of electrode surfaces by leveraging scanning electrochemical probe microscopy (SEPM) techniques, capable of capturing spatially resolved electrochemical information with micro or nanoscale resolution [1]. Correlating this information with the local physicochemical properties of materials, obtained by complementary microscopy and spectroscopy at *identical locations*, opens up new avenues to achieve a comprehensive understanding of property–function relationships. In essence, complex electroactive surfaces are studied as a collection of simpler "single entities" [2], such as individual particles, structural features, defects [3], etc.

The most notable SEPM techniques for correlative electrochemical multi-microscopy are scanning electrochemical microscopy (SECM) [4], scanning ion conductance microscopy (SICM) [5], and scanning electrochemical cell microscopy (SECCM) [6–8]. Although the newest amongst these, SECCM has found the most application, by some margin, due to its inherent advantages for correlative analysis, including direct measurement of the electrochemical reaction of interest, easy access to nanoscale resolution [9–11], and multi-scale capabilities [12–15]. SECCM utilizes a pipette probe filled with an electrolyte, creating a mobile electrochemical droplet cell at the tip for spatially resolved electrochemical measurements [1].

Note: all authors contributed equally to this work.

Built on an open access and easily customizable platform [16], the SECCM format allows easy optical visualization of the probe and surface, which is key to allowing measurements at identical locations across different microscopies. Optical visualization of the probe has been implemented from the earliest use of the technique, e.g. top-view cameras for opaque substrates [17] or inverted microscopes for transparent substrates [18,19], so that the probe can be targeted at a specific region of interest on the sample [17]. Identifiable surface features and the electrolyte footprints left behind serve as a precise marker for subsequent correlative analysis by applying identical location, complementary characterization techniques, e.g., scanning and transmission electron microscopy (SEM, TEM) [20–22], atomic force microscopy (AFM) [23], Raman spectroscopy [23], electron backscatter diffraction (EBSD) [24], and others. *In-situ* optical monitoring of the SECCM experiment has more recently been established and, apart from providing direct visualization of the droplet cell [25], it also offers measurement automation [26,27] and a foundation for the subsequent development of artificial intelligence imaging routines.

An important aspect of SECCM is that mass transport and interfacial reactivity can be treated in detail by finite element method (FEM) modelling [28,29] and, more recently, by simpler analytical expressions [30]. This theoretical knowledge complements practical aspects, such as the effects of iR drop [31], or the placement of the quasi-reference counter electrode inside the pipet probe [32].

In excess of a hundred articles have been published using SECCM in the past three years alone, showcasing its wide adoption in numerous electrochemical studies. This review aims to provide an overview of recent advances in correlative co-located electrochemical multi-microscopy using SECCM to elucidate property–function relationships in electrode materials. Specifically, we focus on the correlation of electrochemical behavior with a range of physicochemical properties that can be obtained through complementary characterization techniques, both *ex situ* and *in situ*. Table 1, towards the end of the article, presents an overview of the complementary techniques discussed herein. We highlight the versatility of this approach by presenting a variety of electrode materials and interfaces relevant to important electrochemical applications (Figure 1). The review begins by exploring the importance of the SECCM meniscus contact to enable correlative analysis. Subsequently, we provide illustrative examples of correlative multi-microscopy studies of 2D materials, polycrystalline extended surfaces, single electrocatalytic particles, battery interfaces and interphases, electrode fabrication and functionalization, and spatially complex electrode structures. Readers may also find other relevant reviews of interest, including those addressing SECCM [7,8] and, more generally, nanoscale electrochemical mapping [1,4,33] and high-throughput nanoelectrochemistry [34].

Advances in understanding and utilizing meniscus contact

The confined nature of the SECCM droplet cell is a key advantage of the technique, as it allows for local investigation of the sample. However, accurate determination of the contact (electrode) area and droplet condition is usually important for reliable measurement data and analysis, e.g., for calculating current density. Typically, the SECCM meniscus contact area is approximately the size of the tip, and various methods have been used to

Table 1

Overview of physicochemical properties of materials obtained by a continuously expanding array of complementary characterization techniques coupled to SECCM, as described in this review.

Property	Characterization technique coupled to SECCM
Footprint area and location	OM, AFM, EM (SEM, TEM)
Meniscus size, state, location	OM (*in-situ* IRM)
Material morphology	OM, AFM, EM (SEM, TEM), DFS
Material topography, thickness, defects	AFM, SR-OS, PL
Crystal structure	EBSD, TEM diffraction
Chemical composition	Raman (SHINERS), EM (EDS, EELS, EFTEM), XPS, SIMS (q-SIMS, ToF-SIMS)
Atomic structure	STEM
Band gap energy	SR-OS

* **Abbreviations:** Optical microscopy (OM), Atomic force microscopy (AFM), Electron microscopy (EM), Scanning electron microscopy (SEM), Transmission electron microscopy (TEM), Interference reflection microscopy (IRM), Dark-field spectroscopy (DFS), Spatially resolved optical spectroscopy (SR-OS), Photoluminescence (PL), Electron backscattered diffraction (EBSD), Shell-isolated nanoparticles for enhanced Raman spectroscopy (SHINERS), Energy-dispersive X-ray spectroscopy (EDS), Electron energy loss spectroscopy (EELS), Energy-filtered transmission electron microscopy (EFTEM), X-ray photoelectron spectroscopy (XPS), Secondary ion mass spectrometry (SIMS), Quadruple SIMS (q-SIMS), Time-of-Flight SIMS (ToF-SIMS), Scanning transmission electron microscopy (STEM).

Figure 1

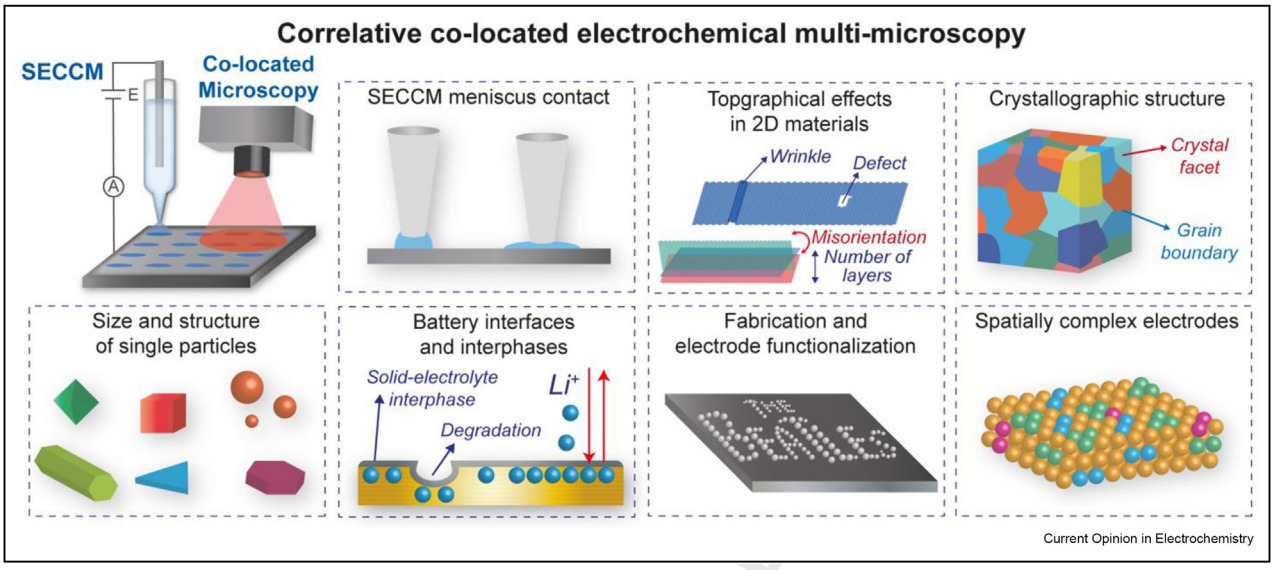

Schematic illustrating the versatility of correlative-electrochemical multi-microscopy approaches based on SECCM and co-located microscopy.

confirm this parameter [6]. Indeed, the electrolyte footprint post−experiment (i.e. meniscus contact area) has been imaged routinely with optical microscopy [35], AFM [36], SEM [21], and even TEM [22]. In certain conditions, such as in alkaline media, the wetting may be more extensive, resulting in a contact area significantly larger than the size of the tip [37,38]. This represents an important consideration when using SECCM, especially when investigating certain types of materials or under specific conditions. To reduce the extent of wetting in such cases, the SECCM pipet can be deployed through an oil layer covering the surface [37−40] but this may not always be practical. The SECCM meniscus wetting in alkaline electrolyte was investigated through the analysis of voltammograms for a pH-independent redox probe, supported by FEM modelling and microscopic imaging of SECCM footprints [41]. This analysis offers a promising method of determining meniscus properties, including the role of evaporation and mass transport, *in-situ* [30,31].

A key advantage of SECCM is its ability to target and encapsulate particles of interest, enabling hundreds or thousands of individual particles or particle aggregates to be investigated in a single experiment. For instance, silica nanospheres of different sizes were individually encapsulated by the SECCM meniscus to study their role as nucleation sites for hydrogen gas bubbles, with the high-throughput capabilities of SECCM enabling detailed and robust statistics [42].

Recently, a hybrid technique combining SECCM with *in-situ* interference reflection microscopy (IRM) was developed [25]. In this configuration, the optical signal is very sensitive to local phase (refractive index) changes, enabling the direct visualization of the meniscus cell during experiments if that is larger than the diffraction limit (ca. 200 nm with commonly used microscope objectives and illumination wavelengths) [25]. Additionally, IRM allows for real-time tracking of phase changes at the electrode-electrolyte interface [25]. This technique has proven effective in detecting electrolyte films of nanoscale thickness, as demonstrated in a study using a pipette-and-droplet reservoir bridging individual nanoparticles (NPs) located close to, but outside, the nominal wetted area [43]. Optical and electron microscopy confirmed an extended electroactive region in this nanofluidics model system. The use of *in-situ* optical microscopy facilitates the development of semi- or fully automated SECCM targeting protocols to probe selected regions of interest within a larger sample area, thereby significantly accelerating experimental workflows. For instance, high-throughput analysis of Li^+ charging/discharging in single TiO_2 NP clusters [26] and electrocatalytic activity of single Au NPs [27] has been successfully demonstrated using this approach, as detailed in following sections.

In addition to targeting specific particles, SECCM allows for probing different parts of a single particle or cluster to reveal its intrinsic electrochemical activity. Hexagonal Co_3O_4 plates were investigated by SECCM by landing on their top surface or their edge, and correlated SEM and AFM measurements were used to extract the kinetics for the oxygen evolution reaction (OER) at each site [44]. Precise nanoscale control of the SECCM

meniscus position and height offers a valuable tool for studying the role of contact resistance (with the substrate electrode), and degree of wetting, in determining the electrochemical performance of single particles (Figure 2a). This approach was employed to investigate the Li^+ charging/discharging kinetics of $LiMn_2O_4$ particles by comparing the response of particles fully wetted by electrolyte (also wetting the current collector) and partly wetted particles (only top contact) [13]. Much faster voltammetric scan rates can be applied in SECCM compared to macroscopic measurements. This feature facilitates the identification of intrinsic kinetic limitations in electrochemical processes, as exemplified in the case of $LiMn_2O_4$ particles supported by detailed physicochemical FEM simulations [13].

Topographical and topological effects on charge transfer in two-dimensional (2D) materials

Topographical variations across an electrode surface can lead to local functionalities that significantly influence charge transfer activity, ion transport, conductivity, and other important phenomena relevant for electrochemical processes. Studies of nanoscale topographical effects in two dimensional (2D) materials, are readily explored using SECCM and characterized by complementary microscopy techniques to reveal their impact on electrochemistry.

SECCM has proven to be a powerful tool for spatially resolved activity measurements in graphene. For instance, monolayer graphene supported on Cu exhibited faster electron-transfer kinetics than bilayer and multilayer graphene for the classical outer-sphere $[Ru(NH_3)_6]^{3+/2+}$ couple, and this finding was grounded on detailed theoretical modelling that revealed that electron-transfer at metal-supported graphene is predominantly adiabatic [45], with the graphene layer(s) modifying the electrostatic potential experienced by the redox couple, and consequently changing the activation barrier for electron transfer.

The $[Ru(NH_3)_6]^{3+/2+}$ process was also investigated at twisted bilayer graphene, formed by stacking atomically thin layers with a small misorientation, to produce a Moiré superlattice (measured by scanning tunnelling microscopy). A strong twist-angle dependence of

Figure 2

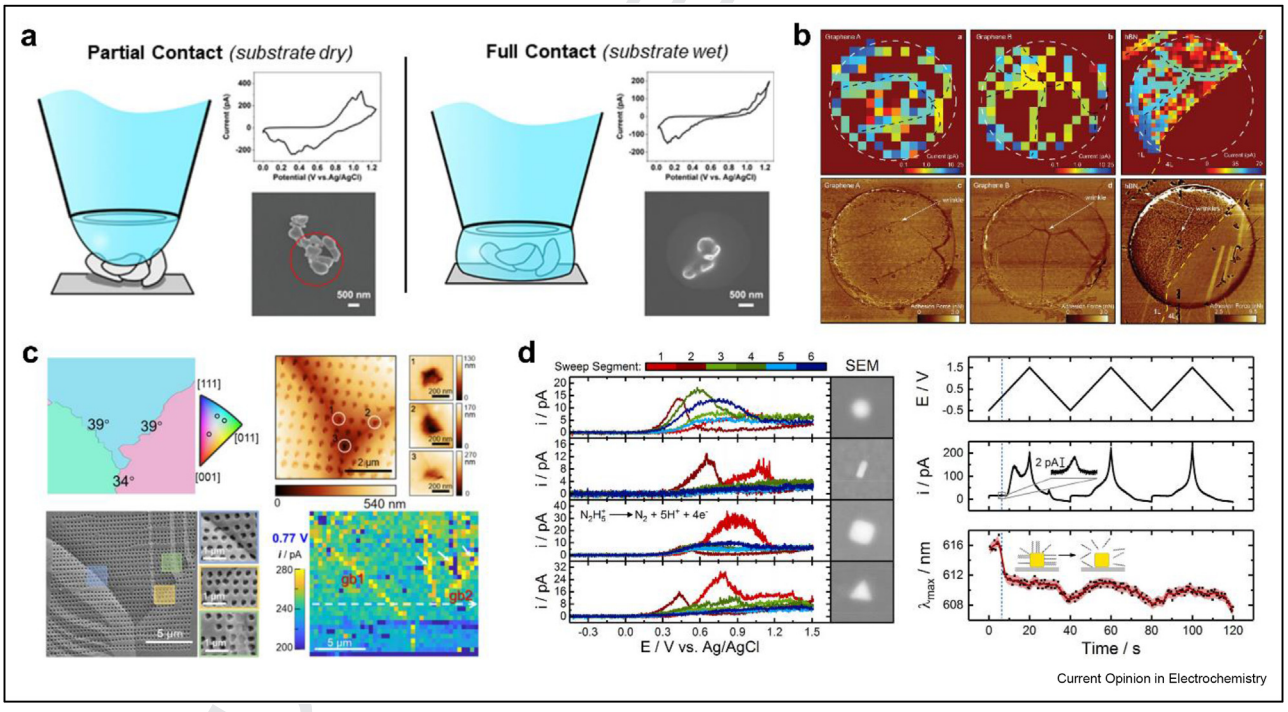

(**a**) Study of $LiMn_2O_4$ particles at different degrees of sample wetting, by means of finely tuning the pipette (and hanging meniscus) vertical position and correlating the electrochemical measurements with SEM of the particles and (where relevant) SECCM footprints. Fully wetting the particles and underlying substrate results in larger voltammogram peak separation than in the case of partially wetting the particles. Reproduced from the study by Tao et al. [13] under CC-BY 4.0. (**b**) SECCM current maps (top) and AFM force maps (bottom) of graphene and hBN layers, linking increased activity to wrinkle and stress areas. Left and middle sections are from a single graphene layer, and right section is from combined one and four-layer hBN regions. Reproduced from the study by Wahab et al. [49] under CC-BY 4.0. (**c**) A co-located SECCM/EBSD/AFM approach to correlate the local Ag dissolution with crystallographic orientations and grain boundary locations, illustrating structure-activity relationships. Reproduced with permission from the study by Wang et al. [62]. Copyright 2022 American Chemical Society. (**d**) Left: SECCM cyclic voltammograms at individual Au NPs of varied shapes. Right: current (middle panel) and *in-situ* optical scattering (bottom panel) measurements during potential cycling (top panel) of Au nanocubes. Reproduced with permission from the study by Saha et al. [27]. Copyright 2023 American Chemical Society. Q5

electron transfer kinetics was discovered that was related to the changes in the electronic structure of the bilayer graphene devices [46]. A further study of twisted trilayer graphene demonstrated that electron transfer rates are influenced by the electronic localization in each atomic layer rather than the overall density of states [47].

SECCM has been instrumental in exploring local proton transport properties within 2D materials, such as defective graphene structures [48]. Recently, it has enabled the discovery of proton transport through defect-free monolayers of graphene and hexagonal boron nitride (hBN) (Figure 2b) [49]. Co-located AFM revealed that this phenomenon occurs at nanoscale wrinkles and others regions with a stressed or curved lattice, which lowers the activation barrier for proton transfer, as revealed by density functional theory (DFT) calculations. Proton transport was also suggested to be fast along the surface of MXenes, such as $Ti_3C_2T_x$ flakes [50], identified by an SECCM study of the pseudocapacitive response of this material through controlled contact of only a small basal plane region of a monolayer flake.

The electrochemical response of single and multiple layers of 2D transition metal dichalcogenides has also been mapped by SECCM. Electron transfer kinetics was found to be dependent on number of layers for several of these materials, associated to a change in band gap and electron tunnelling barrier [36]. Coupling SECCM with field-effect electrostatic manipulation of band alignment demonstrated the effect of charge carrier concentration on heterogeneous electron transfer at few-layer MoS_2 electrodes, as observed using the $[Ru(NH_3)_6]^{3+/2+}$ couple [35].

Several studies have explored the combination of SECCM with photoluminescence measurements to investigate different optoelectronic phenomena in 2D materials, e.g., charge transport and carrier recombination in the vicinity of photoexcited spots in layered WSe_2 [51,52], enhanced photoelectrocatalytic activity at the interface of strained MoS_2/Cu_2O heterostructures [53], and locally increased photocurrents caused by edge-type defects on MoS_2 crystals [54].

Effect of crystallographic structure in extended polycrystalline surfaces on local electrochemical kinetics

Various aspects of electrochemical reactivity, such as the nature of active sites, ion surface adsorption, and degradation, are significantly influenced by the accessible crystallographic facets and grain boundaries on polycrystalline electrode surfaces. Elucidating crystallographic structure-function relationships is thus important for the optimization of electrode materials. SECCM provides an efficient method for locally interrogating a multitude of sites in extended polycrystalline materials, by employing a high-throughput *pseudo-single-crystal* approach to reveal insights into the origin of crystal-dependent electrochemical reactivity in combination with co-located EBSD mapping.

This approach has been successfully applied to image the electrochemical CO_2 reduction reaction (eCO_2RR) on polycrystalline Cu [55], revealing that higher eCO_2RR activity occurs on facets with higher step and kink site density. Similarly, several electrocatalytic and surface processes on polycrystalline Pt were studied within a single SECCM measurement, providing insights into facet-dependent electrochemical performance [56,57]. Local variations of HER kinetics across polycrystalline Ag were correlated to specific crystal facets through spatially resolved Tafel slope analysis [58]. In another study, the OER activity of Co oxy(hydroxide) was found to differ on various facets of the underlying polycrystalline Co electrode [59], which in combination with other characterisation techniques such as X-ray photoelectron spectroscopy (XPS), transmission electron microscopy (TEM), and atom probe tomography allowed for a deeper understanding of OER activity and the composition, structure, and thickness of these materials. The effect of boron-doped diamond terminations on electrochemical activity was determined by SECCM complemented with identical location Raman, AFM, and SEM characterization, both for single-crystal particles and polycrystalline surfaces [60]. Additionally, SECCM-EBSD revealed that the efficiency of benzotriazole as a corrosion inhibitor is dependent on the crystallographic facet of Cu materials [61].

Grain boundaries between crystallographic facets with accumulated defects can also act as hotspots of electrochemical activity. This crucial information can be accessed by high-resolution SECCM, particularly in combination with high angular resolution EBSD to reveal the nature of the grain boundary. For instance, the origin of enhanced eCO_2RR activity at grain boundaries in Au electrodes was linked to surface-terminating dislocations [29]. Similarly, Ag dissolution rate was found to be promoted by the interfacial energy and the density of steps and broken bonds at the grain boundary planes (Figure 2c) [62].

Effect of size and structure on the electrochemical behavior of single NPs

NPs supported on electrodes play an essential role in electrochemistry, especially in electrocatalysis applications. Despite efforts to synthesize well-defined monodisperse NPs, there will be subtle differences in atomic arrangements and surface capping agents (if used) from one NP to another, affecting their surface free energy and reactivity [63]. Probing the structure-activity relationships of single NPs is important, but it

poses inherent challenges due to their small size and complex nature.

SECCM is an ideal technique for performing single-particle electrochemical measurements, achieved by simply bringing the probe into meniscus contact with targeted particles, as discussed above, and reviewed earlier [7,8]. SECCM was employed in combination with a single-particle-on-a-nanoelectrode approach to investigate the OER at individual Co_3O_4 nanocubes [64]. The former technique provided statistics from a large number of measurements, while the latter enabled accelerated stress tests under highly alkaline conditions and high current densities. By employing identical-location electron microscopy, structural transformations of individual nanocubes during electrochemical processes were visualized.

In another study, plasmon resonance was combined with SECCM to reveal local reactive hotspots in Au nanorods during light-assisted electrochemical dissolution [65]. A spectral redshift in dark-field spectroscopy indicated isotropic dissolution of the nanorods, while a blueshift suggested a tip-preferred transformation, which was confirmed with complementary SEM imaging. More recently, SECCM was used to evaluate the catalytic activity across Au NPs with different morphologies (Figure 2d), with *in-situ* optical microscopy aiding in targeting individual NPs for analysis [27]. Correlating SECCM data with optical spectroscopy and TEM showed negligible morphological changes of the Au NPs during operation. Thus, variations in catalytic behavior were attributed to adsorbates or surface restructuring.

The capability of SECCM to isolate and analyze the electrochemical response of single particles has been successfully exploited for various materials, e.g., Au [66,67] and Cu_2O [68]. The electrocatalytic activity of individual Pd NPs was related to distinct crystal planes and strain associated with the particle's shape [69]. Similarly, hematite nanorods with {110} and {001} facets at the tip and body parts, respectively, exhibited face-dependent OER activity [70], as revealed by a correlative SECCM and co-located electron microscopy study.

Battery interfaces and interphases

SECCM is becoming increasingly popular for studying battery-related interfaces and interphases. Successful operation of SECCM with non-aqueous electrolytes and inside a glovebox environment [16,21] has enabled the analysis of micro and nanoscale features of battery materials under working conditions, combined with other characterization techniques.

For instance, charge-discharge measurements of single $LiFePO_4$ particles were performed to evaluate the charge transfer resistance in both aqueous and organic electrolytes [71]. The implementation of a semi-automatic optics-enabled targeted SECCM scanning protocol enabled high-throughput measurements of Li-ion charging/discharging of clusters of TiO_2 NPs by significantly reducing experimental times [26]. Many clusters revealed a relatively high capacity, dependent on the size of individual NPs, under fast charging conditions.

Interfacial structure transformations on Si electrodes were induced and studied by local Li-ion electrochemical cycling using SECCM [72]. Cross sectional analysis of SECCM regions of the electrodes, carefully extracted by Xe^+ plasma-focused ion beam and examined by high-resolution scanning TEM, revealed varying degrees of nanoscale surface degradation, which depended on the crystallographic properties of the Si electrode. In a further study, the effect of the native oxide layer on Si electrodes on the solid-electrolyte interphase (SEI) formation and lithiation reversibility was revealed by SECCM and correlative secondary ion mass spectrometry (SIMS) (Figure 3a). Removing the oxide layer resulted in Li trapping and reduced reversibility [21]. Further insights about the dynamics and intricate composition of the SEI on Si were discovered by coupling SECCM with shell-isolated nanoparticles for enhanced Raman spectroscopy (SHINERS) [73]. The chemical composition of the SEI was found to be strongly dependent on certain experimental conditions by a high-throughput combinatorial electrochemistry experiment, which simultaneously evaluated the effect of charge/discharge cycle, cut-off voltage, and electrolyte solvent.

Controlled fabrication, functionalization, and probing of complex electrode structures

SECCM is a versatile and powerful tool that can provide valuable insights into additional fundamental and applied processes, including controlled fabrication of (nano)structures, local functionalization and patterning of surfaces, as well as the analysis of complex electrode materials with variable composition and porosity. Those applications are greatly enhanced when coupled with complementary co-location microscopy.

Fabrication of well-ordered arrays of Ag NPs (Figure 3b) was achieved by controlling nucleation and growth events by SECCM to yield individual nanoparticles of defined size [20]. Deep understanding of single-nanoparticle formation can be achieved by coupling SECCM with *in-situ* optical microscopy, which enabled the real-time optical monitoring of Ag electrodeposition dynamics with high temporal and spatial resolution [74]. The statistical nature of nucleation and growth processes can be revealed by conducting hundreds of SECCM individual measurements, as demonstrated in the electrochemical formation and dissolution of Au NPs [75].

Figure 3

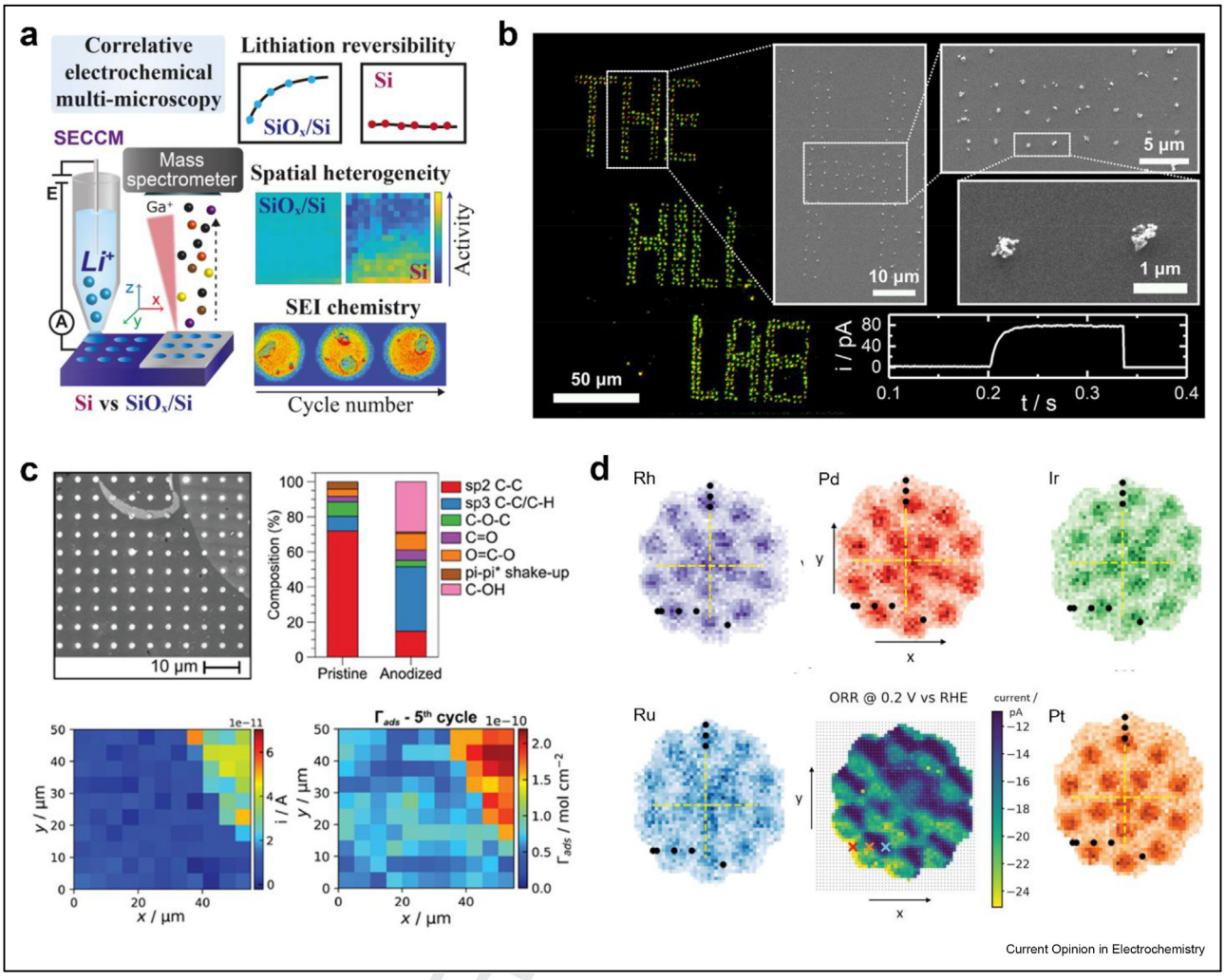

(**a**) Correlative SECCM/SIMS multi-microscopy to reveal interfacial chemistry effects in the electrochemical performances of HF−Si and SiO_x/Si. Reproduced from the study by Xu et al. [21] under CC-BY 4.0. (**b**) Optical dark field scattering and SEM images of Ag NP arrays on ITO, fabricated via SECCM patterning. Reproduced with permission from Rahaman et al. [20]. Copyright 2022 American Chemical Society. (**c**) SEM image of the locally anodized (top right corner of the image) glassy carbon surface, also showing SECCM landing spots; and the relative composition of carbon-based functional groups obtained from C 1s XPS spectra, the ratio of D and G bands (I_D/I_G) obtained from Raman (top). Spatially resolved dopamine oxidation kinetics obtained from SECCM across the pristine and locally anodized areas (bottom). Reproduced from the study by Swinya et al. [23] under CC-BY 4.0. (**d**) Chemical composition and spatially resolved OER activity map obtained by EDS and SECCM on high-entropy alloys. Reproduced from the study by Banko et al. [77] with permission by the authors.

Additionally, SECCM also enabled the local electroless deposition of molecular materials, such as cobaloxime complexes used for photocatalytic HER studies [76].

SECCM has also proven to be a valuable tool for locally introducing chemical functionalities [23] or defects [15] into materials. For instance, anodizing glassy carbon electrodes resulted in the increase of oxygen functionalities and surface roughness, as determined by complementary XPS, energy dispersive X-ray spectroscopy (EDS) and Raman (Figure 3c) [23]. This local modification allowed for the investigation of dopamine adsorption and electron-transfer kinetics at both the modified and bare carbon regions in a single spatially resolved SECCM experiment. SECCM has been applied to reveal the effect of various chemical compositions across a single material such as high-entropy alloy electrocatalysts (Figure 3d). By correlating spatially resolved electrocatalytic activity with EDS mapping, high-activity multi-metal compositions in exemplary systems such as Ru−Rh−Pd−Ir−Pt and Co−Ni−Mo−Pd−Pt were identified [77].

Figure 4

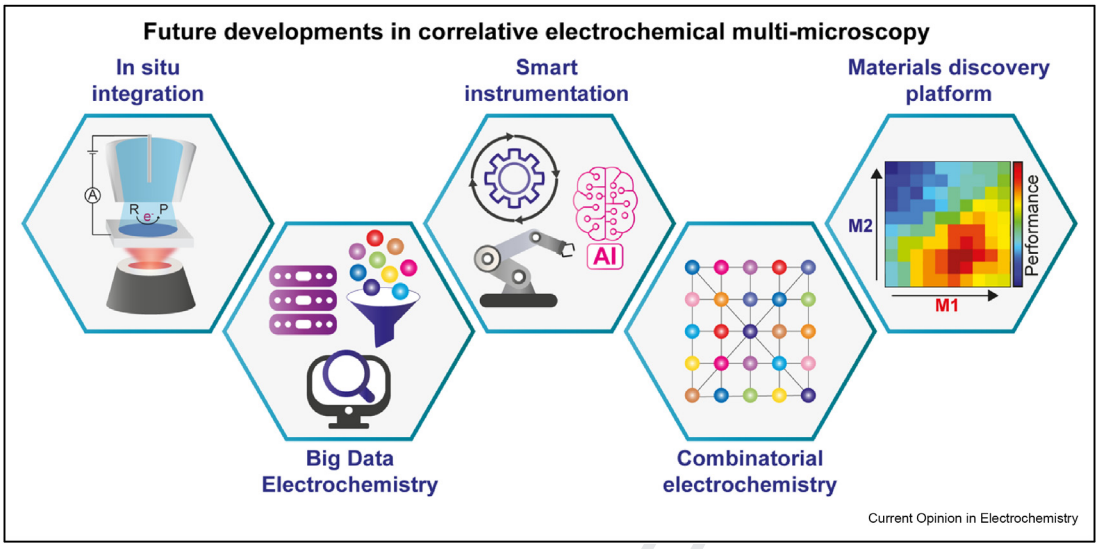

Schematic representation of some future research directions in correlative electrochemical multi-microscopy.

SECCM has further been exploited to study local properties in thin film electrode materials. For instance, coupling SECCM imaging and time-of-flight SIMS (ToF-SIMS) measurements enabled the probing of heterogeneous pitting corrosion of NiO films on Ni interfaces, highlighting Cl^- penetration into the NiO layer at susceptible breakdown sites [78]. The topography of nanostructured $BiVO_4$ thin films was found to control photoelectrochemical activity by coupling SECCM with spatially resolved optical spectroscopy [79], which also allowed simultaneous mapping of absorbance and band gap energy across the thin film material. Correlative SECCM with EDS, XPS and AFM enabled the identification of nanoscale porosity variations across thin films of amorphous MoS_x associated to heterogeneities in electrocatalytic activity [80]. Heterogeneous particle agglomerates of an Fe−N−C catalyst demonstrated similar spatially resolved oxygen reduction reaction (ORR) performance when the activity was normalized by electrochemical surface area, depending on the material porosity [81].

Conclusions and outlook

Correlative electrochemical multi-microscopy, with SECCM at the center, is rapidly emerging as a transformative tool for investigating property−function relationships in electrode materials, impacting many research fields that relate to electrochemistry. In this review, we have highlighted the power of this approach to probe microscale and nanoscale physicochemical properties on a variety of electrode materials and reveal their effect on electrochemical processes by coupling SECCM with complementary co-located characterization techniques (Table 1). This new way of studying electroactive components is set to accelerate the rational design of tailored electrochemical interfaces, unlocking new possibilities across the electrochemistry discipline.

We anticipate significant advances in correlative electrochemical multi-microscopy in the coming years, with several key directions poised to shape the field (as depicted in Figure 4). One direction involves further integration of *in-situ* complementary techniques with SECCM, enabling the dynamic acquisition of chemical and structural information of materials [4] at scales commensurate with SECCM. Techniques from optical spectroscopy to mass spectroscopy should be amenable to integrate with the SECCM platform. Enhancing the throughput of correlative SECCM measurements can also catalyze the field of big data electrochemistry [82]. The development of smart instrumentation, incorporating automatization, robotics, and artificial intelligence [82,83] into both SECCM and complementary techniques will play an important role in minimizing manual input and enabling high-throughput correlative electrochemical multi-microscopy [84]. This approach has the potential to become a premier tool for accelerating mechanistic understanding and automated materials discovery, particularly when used with combinatorial electrochemistry [73], where each SECCM measurement is conducted under different experimental conditions. The future of correlative electrochemical multi-microscopy is bright, introducing a new era of rapid, efficient, and comprehensive research in the field of electrochemical materials.

Declaration of competing interest

The authors declare that they have no known competing financial interests or personal relationships that could have appeared to influence the work reported in this paper.

Data availability

No data was used for the research described in the article.

Acknowledgments

We acknowledge financial support from the European Union's Horizon 2020 research and innovation programme under the Marie Skłodowska-Curie grant agreements no. 101026563 (NANODENDRITE) and no. 812398 (SENTINEL). We also acknowledge UK's Engineering and Physical Sciences Research Council for funding under grant EP/R018820/1 (Crystallisation in the Real World) and grant EP/V037943/1 (Sustainable Chemicals Innovations Enabling Net Carbon Emissions, SCIENCE).

References

Papers of particular interest, published within the period of review, have been highlighted as:

* of special interest
** of outstanding interest

1. Bentley CL, *et al.*: **Nanoscale electrochemical mapping**. *Anal Chem* 2019, **91**:84–108, https://doi.org/10.1021/acs.analchem.8b05235.

2. Baker LA: **Perspective and prospectus on single-entity electrochemistry**. *J Am Chem Soc* 2018, **140**:15549–15559, https://doi.org/10.1021/jacs.8b09747.

3. Cabré MB, Paiva AE, Velický M, Colavita PE, McKelvey K: **Electrochemical detection of isolated nanoscale defects in 2D transition metal dichalcogenides**. *J Phys Chem C* 2022, **126**:11636–11641, https://doi.org/10.1021/acs.jpcc.2c01656.

4. Santana Santos C, Jaato BN, Sanjuán I, Schuhmann W, Andronescu C: **Operando scanning electrochemical probe microscopy during electrocatalysis**. *Chem Rev* 2023, **123**:4972–5019, https://doi.org/10.1021/acs.chemrev.2c00766.

5. Zhu C, Huang K, Siepser NP, Baker LA: **Scanning ion conductance microscopy**. *Chem Rev* 2021, **121**:11726–11768, https://doi.org/10.1021/acs.chemrev.0c00962.

6. Ebejer N, *et al.*: **Scanning electrochemical cell microscopy: a versatile technique for nanoscale electrochemistry and functional imaging**. *Annu Rev Anal Chem* 2013, **6**:329–351, https://doi.org/10.1146/annurev-anchem-062012-092650.

7. Bentley CL, Kang M, Unwin PR: **Scanning electrochemical cell microscopy: new perspectives on electrode processes in action**. *Curr Opin Electrochem* 2017, **6**:23–30, https://doi.org/10.1016/j.coelec.2017.06.011.

8. Wahab OJ, Kang M, Unwin PR: **Scanning electrochemical cell microscopy: a natural technique for single entity electrochemistry**. *Curr Opin Electrochem* 2020, **22**:120–128, https://doi.org/10.1016/j.coelec.2020.04.018.

9. Wahab OJ, Kang M, Meloni GN, Daviddi E, Unwin PR: **Nanoscale visualization of electrochemical activity at indium tin oxide electrodes**. *Anal Chem* 2022, **94**:4729–4736, https://doi.org/10.1021/acs.analchem.1c05168.

10. Kawabe Y, *et al.*: **1T/1H-SnS_2 sheets for electrochemical CO_2 reduction to formate**. *ACS Nano* 2023, **17**:11318–11326, https://doi.org/10.1021/acsnano.2c12627.

11. Tsujiguchi T, *et al.*: **Acceleration of electrochemical CO_2 reduction to formate at the Sn/reduced graphene oxide interface**. *ACS Catal* 2021, **11**:3310–3318, https://doi.org/10.1021/acscatal.0c04887.

12. Tetteh EB, *et al.*: **Zooming-in – visualization of active site heterogeneity in high entropy alloy electrocatalysts using scanning electrochemical cell microscopy**. *Electrochem Sci Adv* 2021, **2**, e2100105, https://doi.org/10.1002/elsa.202100105.

13. Tao B, McPherson IJ, Daviddi E, Bentley CL, Unwin PR: **Multi-scale electrochemistry of lithium manganese oxide ($LiMn_2O_4$): from single particles to ensembles and degrees of electrolyte wetting**. *ACS Sustainable Chem Eng* 2023, **11**:1459–1471, https://doi.org/10.1021/acssuschemeng.2c06075.

14. Bentley CL, Kang M, Unwin PR: **Nanoscale structure dynamics within electrocatalytic materials**. *J Am Chem Soc* 2017, **139**:16813–16821, https://doi.org/10.1021/jacs.7b09355.

15. Hill JW, Fu Z, Tian J, Hill CM: **Locally engineering and interrogating the photoelectrochemical behavior of defects in transition metal dichalcogenides**. *J Phys Chem C* 2020, **124**:17141–17149, https://doi.org/10.1021/acs.jpcc.0c05235.

16. Martín-Yerga D, Kang M, Unwin PR: **Scanning electrochemical cell microscopy in a glovebox: structure-activity correlations in the early stages of solid-electrolyte interphase formation on graphite**. *Chemelectrochem* 2021, **8**:4240–4251, https://doi.org/10.1002/celc.202101161.

17. Lai SCS, Dudin PV, Macpherson JV, Unwin PR: **Visualizing zeptomole (Electro)Catalysis at single nanoparticles within an ensemble**. *J Am Chem Soc* 2011, **133**:10744–10747, https://doi.org/10.1021/ja203955b.

18. Mariano RG, *et al.*: **Thousand-fold increase in O_2 electroreduction rates with conductive MOFs**. *ACS Cent Sci* 2022, **8**:975–982, https://doi.org/10.1021/acscentsci.2c00509.

19. Saha P, Hill JW, Walmsley JD, Hill CM: **Probing electrocatalysis at individual Au nanorods via correlated optical and electrochemical measurements**. *Anal Chem* 2018, **90**:12832–12839, https://doi.org/10.1021/acs.analchem.8b03360.

20. ** Rahman MM, Tolbert CL, Saha P, Halpern JM, Hill CM: **On-demand electrochemical fabrication of ordered nanoparticle arrays using scanning electrochemical cell microscopy**. *ACS Nano* 2022, **16**:21275–21282, https://doi.org/10.1021/acsnano.2c09336.
This article presents a method for patterning substrates with arrays of Ag NPs using SECCM electrodeposition. The material volume is controlled by the charge recorded during the experiment, and the resulting pattern is characterized by optical and electron microscopy.

21. Xu X, *et al.*: **Interfacial chemistry effects in the electrochemical performance of silicon electrodes under lithium-ion battery conditions**. *Small* 2023, e2303442, https://doi.org/10.1002/smll.202303442.

22. Ustarroz J, *et al.*: **Mobility and poisoning of mass-selected platinum nanoclusters during the oxygen reduction reaction**. *ACS Catal* 2018, **8**:6775–6790, https://doi.org/10.1021/acscatal.8b00553.

23. Swinya DL, Martín-Yerga D, Walker M, Unwin PR: **Surface nanostructure effects on dopamine adsorption and electrochemistry on glassy carbon electrodes**. *J Phys Chem C* 2022, **126**:13399–13408, https://doi.org/10.1021/acs.jpcc.2c02801.

24. Bentley CL, Kang M, Unwin PR: **Scanning electrochemical cell microscopy (SECCM) in aprotic solvents: practical considerations and applications**. *Anal Chem* 2020, **92**:11673–11680, https://doi.org/10.1021/acs.analchem.0c01540.

25. ** Valavanis D, *et al.*: **Hybrid scanning electrochemical cell microscopy-interference reflection microscopy (SECCM-IRM): tracking phase formation on surfaces in small volumes**. *Faraday Discuss* 2022, **233**:122–148, https://doi.org/10.1039/d1fd00063b.
This work introduces the hybrid SECCM-IRM technique, which is used to visualize the SECCM-wetted electrode interface via in situ optical microscopy and the use of semi-transparent and conductive substrates. Electrochemical reactions are monitored through the high-throughput SECCM platform, while any phase changes within the meniscus cell are simultaneously highlighted by interference-based optics.

26. ** Tetteh EB, *et al.*: **Fast Li-ion storage and dynamics in TiO_2 nanoparticle clusters probed by smart scanning electrochemical cell microscopy**. *Angew Chem Int Ed* 2023, **62**, e202214493, https://doi.org/10.1002/anie.202214493.
A smart scanning approach is employed to efficiently target clusters and individual TiO_2 particles on an optically-transparent substrate.

SECCM reveals fast Li^+ storage dynamics, while operating under battery-relevant conditions, inside a glovebox.

27. Saha P, Rahman MM, Hill CM: **Electrocatalysis at individual colloidal nanoparticles: a quantitative survey of four geometries via electrochemical cell microscopy**. *J Phys Chem C* 2023, **127**:9059–9066, https://doi.org/10.1021/acs.jpcc.3c01427.

28. Snowden ME, *et al.*: **Scanning electrochemical cell microscopy: theory and experiment for quantitative high resolution spatially-resolved voltammetry and simultaneous ion-conductance measurements**. *Anal Chem* 2012, **84**:2483–2491, https://doi.org/10.1021/ac203195h.

29. * Mariano RG, *et al.*: **Microstructural origin of locally enhanced CO_2 electroreduction activity on gold**. *Nat Mater* 2021, **20**: 1000–1006, https://doi.org/10.1038/s41563-021-00958-9.
This work explores CO_2 electroreduction across different grains and grain boundaries on polycrystalline gold. SECCM and EBSD highlight locally enhanced activity at surface-terminating dislocations.

30. Anderson KL, Edwards MA: **Evaluating analytical expressions for scanning electrochemical cell microscopy (SECCM)**. *Anal Chem* 2023, **95**:8258–8266, https://doi.org/10.1021/acs.analchem.3c00216.

31. Blount B, Juarez G, Wang Y, Ren H: **iR drop in scanning electrochemical cell microscopy**. *Faraday Discuss* 2022, **233**: 149–162, https://doi.org/10.1039/d1fd00046b.

32. Bentley CL, Perry D, Unwin PR: **Stability and placement of Ag/AgCl quasi-reference counter electrodes in confined electrochemical cells**. *Anal Chem* 2018, **90**:7700–7707, https://doi.org/10.1021/acs.analchem.8b01588.

33. Xu J, Gao H, Wang F, Zhou M: **Nanoscale electrochemical approaches to probing single atom electrocatalysts**. *Curr Opin Electrochem* 2023, **39**, 101299, https://doi.org/10.1016/j.coelec.2023.101299.

34. Xu X, *et al.*: **The new era of high-throughput nano-electrochemistry**. *Anal Chem* 2023, **95**:319–356, https://doi.org/10.1021/acs.analchem.2c05105.

35. Maroo S, Yu Y, Taniguchi T, Watanabe K, Bediako DK: **Decoupling effects of electrostatic gating on electronic transport and interfacial charge-transfer kinetics at few-layer molybdenum disulfide**. *ACS Nanoscience Au* 2023, **3**:204–210, https://doi.org/10.1021/acsnanoscienceau.2c00064.

36. Brunet Cabré M, Paiva AE, Velický M, Colavita PE, McKelvey K: **Electrochemical kinetics as a function of transition metal dichalcogenide thickness**. *Electrochim Acta* 2021, **393**, 139027, https://doi.org/10.1016/j.electacta.2021.139027.

37. Mefford JT, *et al.*: **Correlative operando microscopy of oxygen evolution electrocatalysts**. *Nature* 2021, **593**:67–73, https://doi.org/10.1038/s41586-021-03454-x.

38. Shkirskiy V, *et al.*: **Nanoscale scanning electrochemical cell microscopy and correlative surface structural analysis to map anodic and cathodic reactions on polycrystalline Zn in acid media**. *J Electrochem Soc* 2020, **167**:41507, https://doi.org/10.1149/1945-7111/ab739d.

39. Li Y, Morel A, Gallant D, Mauzeroll J: **Correlating corrosion to surface grain orientations of polycrystalline aluminum alloy by scanning electrochemical cell microscopy**. *ACS Appl Mater Interfaces* 2022, **14**:47230–47236, https://doi.org/10.1021/acsami.2c12813.

40. Li Y, Morel A, Gallant D, Mauzeroll J: **Controlling surface contact, oxygen transport, and pitting of surface oxide via single-channel scanning electrochemical cell microscopy**. *Anal Chem* 2022, **94**:14603–14610, https://doi.org/10.1021/acs.analchem.2c02459.

41. Varhade S, *et al.*: **Elucidation of alkaline electrolyte-surface interaction in SECCM using a pH-independent redox probe**. *Electrochim Acta* 2023, **460**:142548, https://doi.org/10.1016/j.electacta.2023.142548.

42. Deng X, *et al.*: **Direct measuring of single-heterogeneous bubble nucleation mediated by surface topology**. *Proc Natl Acad Sci USA* 2022, **119**, e2205827119, https://doi.org/10.1073/pnas.2205827119.

43. Godeffroy L, Shkirskiy V, Noël J-M, Lemineur J-F, Kanoufi F: **Fuelling electrocatalysis at a single nanoparticle by ion flow in a nanoconfined electrolyte layer**. *Faraday Discuss* 2023, https://doi.org/10.1039/D3FD00032J.

44. Varhade S, *et al.*: **Crystal plane-related oxygen-evolution activity of single hexagonal Co_3O_4 spinel particles**. *Chem Eur J* 2023, **29**, e202203474, https://doi.org/10.1002/chem.202203474.

45. Liu DQ, *et al.*: **Adiabatic versus non-adiabatic electron transfer at 2D electrode materials**. *Nat Commun* 2021, **12**:7110, https://doi.org/10.1038/s41467-021-27339-9.

46. * Yu Y, *et al.*: **Tunable angle-dependent electrochemistry at twisted bilayer graphene with moire flat bands**. *Nat Chem* 2022, **14**:267–273, https://doi.org/10.1038/s41557-021-00865-1.
This work illustrates how SECCM can locally probe electronic properties of 2D materials, revealing the angle-dependent electrochemistry that arises when twisting stacked layers of graphene.

47. Zhang K, *et al.*: **Anomalous interfacial electron-transfer kinetics in twisted trilayer graphene caused by layer-specific localization**. *ACS Cent Sci* 2023, **9**:1119–1128, https://doi.org/10.1021/acscentsci.3c00326.

48. Bentley CL, Kang M, Bukola S, Creager SE, Unwin PR: **High-resolution ion-flux imaging of proton transport through Graphene|Nafion membranes**. *ACS Nano* 2022, **16**: 5233–5245, https://doi.org/10.1021/acsnano.1c05872.

49. ** Wahab OJ, *et al.*: **Proton transport through nanoscale corrugations in two-dimensional crystals**. *Nature* 2023, **620**: 782–786, https://doi.org/10.1038/s41586-023-06247-6.
This work investigates local proton transport at structural complex sites in graphene and hexagonal boron nitride 2D membranes. SECCM and co-located AFM suggest that nanoscale wrinkles and other areas of strain modulate proton permeability.

50. * Brunet Cabré M, *et al.*: **Isolation of pseudocapacitive surface processes at monolayer MXene flakes reveals delocalized charging mechanism**. *Nat Commun* 2023, **14**:374, https://doi.org/10.1038/s41467-023-35950-1.
This article reveals the surface charging behaviour of MXene flakes, probed by SECCM and complementary microscopies. Fast proton transport takes place across the surface of a flake, although only a portion of it is contacted by the SECCM meniscus.

51. Tolbert CL, Hill CM: **Electrochemically probing exciton transport in monolayers of two-dimensional semiconductors**. *Faraday Discuss* 2022, **233**:163–174, https://doi.org/10.1039/d1fd00052g.

52. Hill JW, Hill CM: **Directly visualizing carrier transport and recombination at individual defects within 2D semiconductors**. *Chem Sci* 2021, **12**:5102–5112, https://doi.org/10.1039/d0sc07033e.

53. Zheng H, *et al.*: **Strain tuned efficient heterostructure photoelectrodes**. *Chin Chem Lett* 2022, **33**:1450–1454, https://doi.org/10.1016/j.cclet.2021.08.062.

54. Strange LE, *et al.*: **Investigating the redox properties of two-dimensional MoS_2 using photoluminescence spectroelectrochemistry and scanning electrochemical cell microscopy**. *J Phys Chem Lett* 2020, **11**:3488–3494, https://doi.org/10.1021/acs.jpclett.0c00769.

55. Wahab OJ, Kang M, Daviddi E, Walker M, Unwin PR: **Screening surface structure-electrochemical activity relationships of copper electrodes under CO_2 electroreduction conditions**. *ACS Catal* 2022, **12**:6578–6588, https://doi.org/10.1021/acscatal.2c01650.

56. Gaudin LF, Kang M, Bentley CL: **Facet-dependent electrocatalysis and surface electrochemical processes on polycrystalline platinum**. *Electrochim Acta* 2023, **450**:142223, https://doi.org/10.1016/j.electacta.2023.142223.

57. Wang Y, Li M, Ren H: **Voltammetric mapping of hydrogen evolution reaction on Pt locally via scanning electrochemical cell microscopy**. *ACS Meas. Sci. Au* 2022, **2**:304–308, https://doi.org/10.1021/acsmeasuresciau.2c00012.

58. Wang Y, Li M, Gordon E, Ren H: **Mapping the kinetics of hydrogen evolution reaction on Ag via pseudo-single-crystal**

scanning electrochemical cell microscopy. *Chin J Catal* 2022, **43**:3170–3176, https://doi.org/10.1016/S1872-2067(22)64158-5.

59. Luan C, *et al.*: **Linking composition, structure and thickness of CoOOH layers to oxygen evolution reaction activity by correlative microscopy**. *Angew Chem Int Ed* 2023, **62**, e202305982, https://doi.org/10.1002/anie.202305982.

60. Ando T, *et al.*: **Nanoscale reactivity mapping of a single-crystal boron-doped diamond particle**. *Anal Chem* 2021, **93**: 5831–5838, https://doi.org/10.1021/acs.analchem.1c00053.

61. Daviddi E, *et al.*: **Screening the surface structure-dependent action of a benzotriazole derivative on copper electrochemistry in a triple-phase nanoscale environment**. *J Phys Chem C* 2022, **126**:14897–14907, https://doi.org/10.1021/acs.jpcc.2c04494.

62. Wang Y, Li M, Gordon E, Ye Z, Ren H: **Nanoscale colocalized electrochemical and structural mapping of metal dissolution reaction**. *Anal Chem* 2022, **94**:9058–9064, https://doi.org/10.1021/acs.analchem.2c01283.

63. Kim BH, *et al.*: **Critical differences in 3D atomic structure of individual ligand-protected nanocrystals in solution**. *Science* 2020, **368**:60–67, https://doi.org/10.1126/science.aax3233.

64. Quast T, *et al.*: **Single particle nanoelectrochemistry reveals the catalytic oxygen evolution reaction activity of Co_3O_4 nanocubes**. *Angew Chem Int Ed* 2021, **60**:23444–23450, https://doi.org/10.1002/anie.202109201.

65. Al-Zubeidi A, *et al.*: **D-band holes react at the tips of gold nanorods**. *J Phys Chem Lett* 2023, **14**:5297–5304, https://doi.org/10.1021/acs.jpclett.3c00997.

66. * Jeong S, *et al.*: **Unraveling the structural sensitivity of CO_2 electroreduction at facet-defined nanocrystals via correlative single-entity and macroelectrode measurements**. *J Am Chem Soc* 2022, **144**:12673–12680, https://doi.org/10.1021/jacs.2c02001.
In this article, many Au NPs of different morphologies are individually probed with SECCM, and a facet-dependent electrocatalytic activity for CO_2RR is identified, aided by co-located electron microscopy.

67. Choi M, *et al.*: **Probing single-particle electrocatalytic activity at facet-controlled gold nanocrystals**. *Nano Lett* 2020, **20**: 1233–1239, https://doi.org/10.1021/acs.nanolett.9b04640.

68. Shan Y, *et al.*: **Surface facets dependent oxygen evolution reaction of single Cu_2O nanoparticles**. *Chin Chem Lett* 2022, **33**:5158–5161, https://doi.org/10.1016/j.cclet.2022.03.010.

69. Zhao J, *et al.*: **Exploring the strain effect in single particle electrochemistry using Pd nanocrystals**. *Angew Chem Int Ed* 2023, **62**, e202304424, https://doi.org/10.1002/anie.202304424.

70. Li M, Ye KH, Qiu W, Wang Y, Ren H: **Heterogeneity between and within single hematite nanorods as electrocatalysts for oxygen evolution reaction**. *J Am Chem Soc* 2022, **144**: 5247–5252, https://doi.org/10.1021/jacs.2c00506.

71. Yamamoto T, *et al.*: **Characterization of the depth of discharge-dependent charge transfer resistance of a single $LiFePO_4$ particle**. *Anal Chem* 2021, **93**:14448–14453, https://doi.org/10.1021/acs.analchem.1c02851.

72. Martín-Yerga D, *et al.*: **Link between anisotropic electrochemistry and surface transformations at single-crystal silicon electrodes: implications for lithium-ion batteries**. *Nat Sci* 2023, **3**, e20210607, https://doi.org/10.1002/ntls.20210607.

73. ** Martin-Yerga D, *et al.*: **Dynamics of solid-electrolyte interphase formation on silicon electrodes revealed by combinatorial electrochemical screening**. *Angew Chem Int Ed* 2022, **61**, e202207184, https://doi.org/10.1002/anie.202207184.
This article demonstrates how SECCM and correlated microscopies can be used to screen a range of experimental conditions. Local SEI formation on Si electrodes under Li cycling conditions is studied with the help of SEM and surface-enhanced Raman microscopy.

74. Ciocci P, *et al.*: **Optical super-localisation of single nanoparticle nucleation and growth in nanodroplets**. *Chemelectrochem* 2023, **10**, e202201162, https://doi.org/10.1002/celc.202201162.

75. Bernal M, *et al.*: **A microscopic view on the electrochemical deposition and dissolution of Au with scanning electrochemical cell microscopy – Part I**. *Electrochim Acta* 2023, **445**:142023, https://doi.org/10.1016/j.electacta.2023.142023.

76. Oswald E, *et al.*: **Cobaloxime complex salts: synthesis, patterning on carbon nanomembranes and heterogeneous hydrogen evolution studies**. *Chem Eur J* 2021, **27**: 16896–16903, https://doi.org/10.1002/chem.202102778.

77. * Banko L, *et al.*: **Microscale combinatorial libraries for the discovery of high-entropy materials**. *Adv Mater* 2023, **35**, 2207635, https://doi.org/10.1002/adma.202207635.
In this work, the electrocatalytic activity of high-entropy alloy samples is mapped at the nanoscale using SECCM and EDX, with the aim to establishing material property libraries.

78. Li M, *et al.*: **Stochastic local breakdown of oxide film on Ni from identical-location imaging: one single site at a time**. *Nano Lett* 2022, **22**:6313–6319, https://doi.org/10.1021/acs.nanolett.2c02018.

79. Mena-Morcillo E, van der Zalm J, Chen A: **Spatially resolved optical spectroscopic measurements with simultaneous photoelectrochemical mapping using scanning electrochemical probe microscopy**. *J Phys Chem Lett* 2023, **14**: 4600–4606, https://doi.org/10.1021/acs.jpclett.3c00603.

80. Bentley CL, *et al.*: **Correlating the local electrocatalytic activity of amorphous molybdenum sulfide thin films with microscopic composition, structure, and porosity**. *ACS Appl Mater Interfaces* 2020, **12**:44307–44316, https://doi.org/10.1021/acsami.0c11759.

81. Limani N, *et al.*: **Scrutinizing intrinsic oxygen reduction reaction activity of a Fe–N–C catalyst via scanning electrochemical cell microscopy**. *Chemelectrochem* 2023, **10**, e202201095, https://doi.org/10.1002/celc.202201095.

82. Coelho LB, *et al.*: **Probing the randomness of the local current distributions of 316 L stainless steel corrosion in NaCl solution**. *Corrosion Sci* 2023, **217**:111104, https://doi.org/10.1016/j.corsci.2023.111104.

83. Li R, *et al.*: **Unsupervised Analysis of Optical Imaging Data for the Discovery of Reactivity Patterns in Metal Alloy**. *Small Methods* 2023, e2300214, https://doi.org/10.1002/smtd.202300214.

84. Godeffroy L, *et al.*: **Bridging the gap between single nanoparticle imaging and global electrochemical response by correlative microscopy assisted by machine vision**. *Small Methods* 2022, **6**, 2200659, https://doi.org/10.1002/smtd.202200659.